Scientific Article

Lung and Liver Stereotactic Body Radiation Therapy During Mechanically Assisted Deep Inspiration Breath-Holds: A Prospective Feasibility Trial

Loïc Vander Veken, MD, PhD,[a,b,]* Geneviève Van Ooteghem, MD, PhD,[a,b] Benoît Ghaye, MD, PhD,[c] Ariane Razavi, MSc,[b] David Dechambre, MSc,[b] and Xavier Geets, MD, PhD[a,b]

[a]UCLouvain, Institut de Recherche Experimentale et Clinique (IREC), Center of Molecular Imaging, Radiotherapy and Oncology (MIRO), Brussels, Belgium; [b]Radiation Oncology Department, Cliniques Universitaires Saint-Luc, Brussels, Belgium; and [c]Radiology Department, Cliniques Universitaires Saint-Luc, Brussels, Belgium

Purpose: Radiation therapy for tumors subject to breathing-related motion during breath-holds (BHs) has the potential to substantially reduce the irradiated volume. Mechanically assisted and noninvasive ventilation (MANIV) could ensure the target repositioning accuracy during each BH while facilitating treatment feasibility through oxygen supplementation and a perfectly replicated mechanical support. However, there is currently no clinical evidence substantiating the use of MANIV-induced BH for moving tumors. The aim of this work was, therefore, to evaluate the technique's performance under real treatment conditions.

Methods and Materials: Patients eligible for lung or liver stereotactic body radiation therapy were prospectively included in a single-arm trial. The primary endpoint corresponded to the treatment feasibility with MANIV. Secondary outcomes comprised intrafraction geometric uncertainties extracted from real-time imaging, tolerance to BH, and treatment time.

Results: Treatment was successfully delivered in 92.9% (13/14) of patients: 1 patient with a liver tumor was excluded because of a mechanically induced gastric insufflation displacing the liver cranially by more than 1 cm. In the left-right/anteroposterior/craniocaudal directions, the recalculated safety margins based on intrafraction positional data were 4.6 mm/5.1 mm/5.6 mm and 4.7 mm/7.3 mm/5.9 mm for lung and liver lesions, respectively. Compared with the free-breathing internal target volume and midposition approaches, the average reduction in the planning target volume with MANIV reached $-47.2\% \pm 15.3\%$, $P < .001$, and $-29.4\% \pm 19.2\%$, $P = .007$, for intrathoracic tumors and $-23.3\% \pm 12.4\%$, $P < .001$, and $-9.3\% \pm 15.3\%$, $P = .073$, for upper abdominal tumors, respectively. For 1 liver lesion, large caudal drifts of occasionally more than 1 cm were measured. The total slot time was 53.1 ± 10.6 minutes with a BH comfort level of $80.1\% \pm 10.6\%$.

Conclusions: MANIV enables high treatment feasibility within a nonselected population. Accurate intrafraction tumor repositioning is achieved for lung tumors. Because of occasional intra-BH caudal drifts, pretreatment assessment of BH stability for liver lesions is, however, recommended.

Research data are stored in an institutional repository and will be shared on request to the corresponding author.

*Corresponding author: Loïc Vander Veken, MD, PhD; Email: loic.vanderveken@uclouvain.be

Introduction

Respiratory motion is a major source of geometric uncertainties encountered during the irradiation of thoracic and upper abdominal lesions. As a consequence, radiation therapy for these tumor locations requires dedicated motion management strategies.[1]

Several motion mitigation techniques have been designed to compensate for tumor movement in free breathing. The first approach aims at defining an internal target volume (ITV) that encompasses all tumor positions during the respiratory cycle. The ITV is then dilated by an additional safety margin to account for other error sources.[2] Because of its ease of implementation, this technique is the most widespread but has the disadvantage of resulting in a larger irradiated volume.[3,4] Alternatively, the planning target volume (PTV) can be probabilistically constructed where the uncertainties contributions are summed in quadrature.[5,6] It enables to reduce the PTV volume by 12% to 26% compared with the PTV derived from the ITV (PTV_{ITV}).[6-9] However, these techniques have the same methodological weakness of neglecting the breathing-related motion amplitude variability throughout the treatment.[10] By contrast, motion-synchronized irradiation techniques, such as gating and tracking, continuously adapt the beam delivery to the fluctuations of the respiratory pattern. Commercially available solutions for these sophisticated methods require on-board imaging systems that enable real-time positional monitoring of the tumor.[11] These devices are not available on a conventional linear accelerator (linac), which explains at least partially why these techniques are only performed in a minority of radiation therapy centres.[3,4]

A workaround to this complex issue consists of irradiating the lesion during voluntary breath-holds (BHs), with the ultimate objective of freezing its motion.[12] However, recent evidence has highlighted the possibility of supracentimetric intra-BH residual tumor motion despite the use of guidance systems with external surrogates.[13-15] This raises the question of the need to incorporate real-time imaging of the internal anatomy during beam delivery. Furthermore, the treatment completion requires multiple and successive BHs. The feasibility of such an exercise may, therefore, be compromised by the poor general condition of a patient with comorbidity.[16]

BH could potentially be enhanced through mechanically assisted and noninvasive ventilation (MANIV). This technique actively modulates breathing motion without any prior sedation.[17-20] It induces reproducible deep inspiration BHs (DIBHs) driven by positive pressure with oxygen-enriched air[17,21] while cyclically dropping the pressure to allow the patient to exhale. The mechanical support and oxygen supplementation reduce the work of breathing and improve tolerance to apneas, respectively. Moreover, the perfect replication of the high-pressure level would ensure positional reproducibility (mean position of the BH plateau) and stability (range of positions of the BH plateau) of the target during each DIBH. Nevertheless, to our knowledge, there is no clinical trial investigating the combination of DIBH and mechanical ventilation in patients with internal tumors subject to breathing motion. Indeed, the available data involve healthy volunteers in the environment of a magnetic resonance imaging[18,19] machine and patients with breast cancer.[21] The aim of this study was, therefore, to evaluate, in candidates for lung or liver stereotactic body radiation therapy (SBRT), MANIV performances in terms of treatment feasibility and irradiation accuracy, to our knowledge, for the first time, under real treatment conditions. Other critical aspects of the technique viability in routine, such as patients' tolerance and treatment time, were also assessed.

Methods and Materials

Study design and participants

As shown in Fig. 1, a prospective, single-arm, feasibility trial was conducted. Patients over 18 years old with lung or liver neoplasia eligible for SBRT were included. The only exclusion criterion was a history of spontaneous and idiopathic pneumothorax. The study was approved by the ethics committee of Cliniques Universitaires Saint-Luc (Belgian register number: BE403202043332). All participants signed an informed consent document before their enrollment.

Procedures

A gold fiducial (0.75 mm × 10 mm or 0.5 × 10 mm, Visicoil) was anchored percutaneously into the lung tumors by an interventional radiologist to ensure their visualization on intrafraction images. Regarding liver malignancies, 1 lesion was enhanced by Lipidodol (Guerbet, FRA) injection and 3 were tagged with Spi (0.36 × 4 mm, Balt, FRA) radiopaque markers to facilitate the online cone beam computed tomography (CT)-based repositioning. The remaining patients did not undergo a specific procedure, but for 6 of them, surgical clips were present in the tumor vicinity.

A 3-dimensional (3D)-CT image during a mechanically induced DIBH and a 4-dimensional-CT image in free-breathing were acquired for each patient.

As shown in Fig. 2, the treatment workflow involved first the connection to the mechanical ventilator (Bellavista 1000, Vyaire Medical) in adaptive ventilation mode during which the patient continued to breathe freely but received oxygenated air (FiO_2 at 60%). The adaptive
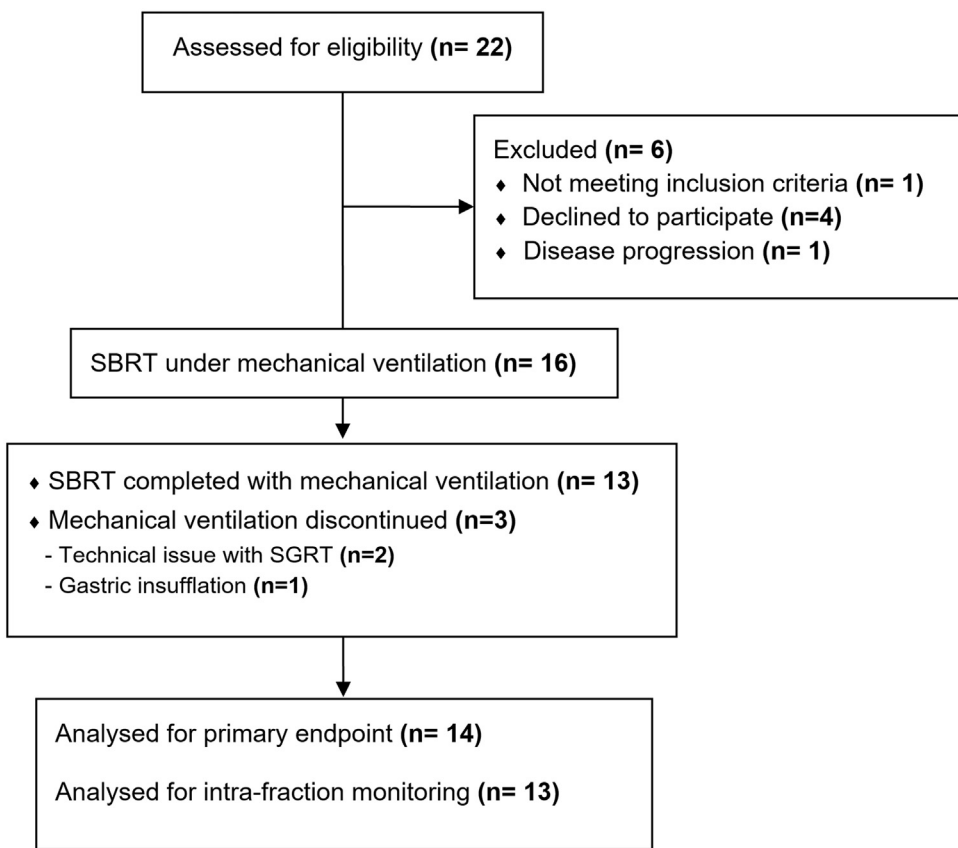
Figure 1 Study flow chart.
Abbreviations: SBRT = stereotactic body radiation therapy; SGRT = surface guided radiation therapy.
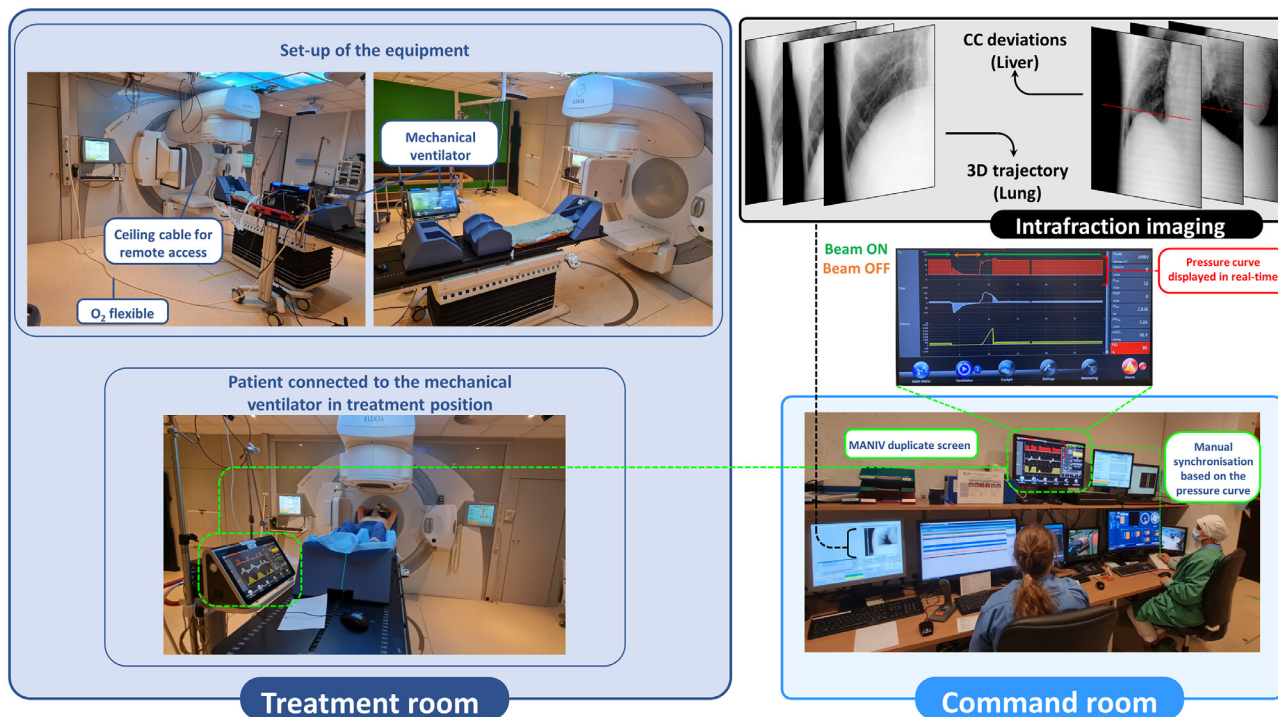

Figure 2 Illustration of the treatment workflow with mechanical ventilation.
Abbreviations: CC = craniocaudal; MANIV = mechanically assisted and noninvasive ventilation.

pressure release ventilation mode was then engaged: a high-pressure level triggered an inspiration and constrained the apnea maintenance for a predefined duration. The pressure then fell automatically to a low level, allowing the patient to exhale before the cycle started again. The irradiation time windows corresponded to the DIBH plateaus, and the beam was interrupted during each expiratory and inspiratory phases. Further details are provided in the supplementary material.

Delineation

For liver lesions, a gross tumor volume (GTV)-to-clinical target volume (CTV) margin of 5 mm was applied, whereas no GTV-to-CTV expansion was used for lung tumors.

On the 3D-CT image acquired during a MANIV-induced DIBH, the PTV_{MANIV} was created using empirical safety margins of 7 mm in all directions.

On the mid-position (MidP) CT image, the PTV_{MidP} was generated according to the van Herk formula[22]:

$$M = \alpha \cdot \sqrt{\Sigma^2_{Delineation} + \Sigma^2_{Setup} + \Sigma^2_{Baseline\ shift} + \Sigma^2_{motion}}$$
$$+ \beta \cdot \sqrt{\sigma^2_{Penumbra} + \sigma^2_{Setup} + \sigma^2_{Baseline\ shift} + \sigma^2_{motion}}$$
$$- \beta \cdot \sigma_{Penumbra}$$

With the exception of σ_{motion}, the systematic (Σ) and random (σ) uncertainties were population-based and in line with the literature.[23,24] Their values corresponded to those used in our institution in clinical routine. According to our institutional procedure, the α and β parameter values were 2.5 and 1.64, respectively. A detailed description is given in Table E1.

The ITV was constructed by the union of the GTVs or CTVs among all 4-dimensional-CT phases for lung and liver tumors, respectively. The additional ITV-to-PTV_{ITV} margin was derived from the aforementioned formula by removing the motion contribution as follows: $\sigma_{motion} = 0$ and $\Sigma_{motion} = 0$.

Treatment planning

The treatment plans were made in Raystation (Raysearsch Lab, version 12a) and consisted of 2 to 4 arcs using a volumetric modulated arc therapy (VMAT) technique with 6-MV photons. The dose was calculated by a collapsed cone convolution algorithm. Planning objectives for target coverage were the following: D95% (dose received by 95% of the PTV volume) equal to 100% of the prescription dose and D_{max} between 110% and 140% of the prescribed dose. For dosimetric comparison purposes, new plans considering the PTV_{MANIV} (with recalculated

margins based on intrafraction data), PTV_{ITV}, and PTV_{MidP} as target volumes were de novo reoptimized created by the same medical physicist. The dose constraints used as clinical goals during the plan optimization are detailed in the study by Diez et al.[25]

Intrafraction motion analysis

Intrafraction cone beam CTs were acquired during irradiation with a maximum frame rate of 5.5 Hz. The intrapulmonary fiducials were tracked on these 2-dimensional (2D) images by an in-house template-based matching algorithm yielding their center of mass co-ordinates. When present, the hepatic radiopaque markers were not visible on the cone beam CT frames. Therefore, the craniocaudal (CC) position of the right diaphragmatic dome (RDD) was selected as surrogate and detected by an in-house gradient-based algorithm. For 1 patient, it was not possible to accurately identify the RDD because of its subcardiac location, the intense noise, and the irregularly shaped cirrhotic liver. Results provided by the flagging tools were visually inspected on each image and manually corrected, if necessary.

The 3D fiducial position was predicted from its 2D co-ordinates, thanks to a probabilistic model based on the optimization of a 3D Gaussian probability density function.[26] For the nonimplanted lung lesion (patient 6), because of the limited range of gantry angles over which the radiopaque structure could be spotted (arc length from 30° to 40°), the baseline shift in the left-right (LR) and anteroposterior (AP) directions may not be properly evaluated, especially along the main KV imager axis.[27] Thus, only continuous monitoring of craniocaudal deviations was considered.

A summary of the intrafraction imaging procedures is provided in Table E2, and details about intrafraction uncertainties recalculation are explained in the supplementary material (Fig. E6 and Table E4). The safety margin was finally derived from the following formula:

$$M = \alpha \cdot \sqrt{\Sigma^2_{Delineation} + \Sigma^2_{Setup} + \Sigma^2_{Baseline\ shift}}$$
$$+ \beta \cdot \sqrt{\sigma^2_{Penumbra} + \sigma^2_{Setup} + \sigma^2_{Baseline\ shift} + \sigma^2_{motion}}$$
$$- \beta \cdot \sigma_{Penumbra}$$

The values for delineation, setup, and penumbra were identical to those used for PTV_{ITV} and PTV_{MidP}.

Outcomes

The primary outcome corresponded to treatment feasibility defined as the ratio of the patients successfully treated to those initially scheduled for treatment with

MANIV. Treatment discontinuations unrelated to poor DIBH compliance or to technical/medical issues with the mechanical ventilator were not considered as MANIV failures. Secondary outcomes included treatment tolerance, treatment time, PTV volumes, and dose to OARs. The global tolerance was assessed after each fraction through a Likert scale (1 = very poor, 2 = poor, 3 = neutral, 4 = good, and 5 = excellent). The DIBH-related tolerance was measured with a visual analog scale, with the minimum and maximum values corresponding to very poor and perfect level of comfort, respectively.

Statistical analyses

Considering a poor and high feasibility threshold of 70% (p_0) and 95% (p_1), respectively, and anticipating a dropout of 10%, 16 patients should be included ($\alpha_{one-sided}$ = 5%, β = 20%).[28] The 95% confidence interval excludes p_0, including the worthwhile p_1 value if at least 13 out of 14 patients complete their treatment with MANIV. The low feasibility limit was derived from the INHALE trial.[16]

Regarding secondary outcomes, continuous variables were compared by a 2-tailed paired t test or a Wilcoxon test in case of Gaussian (Shapiro-Wilk test) or non-Gaussian distribution, respectively.

As part of the dosimetric analysis, the multiple statistical tests introduced a nonnegligible probability of false positives. The false discovery rate was thus controlled by the Benjamini and Hochberg's method.[29]

Statistical analyses were performed in SPSS 27 (IBM).

Results

From May 2021 to January 2023, 16 patients were included. The baseline characteristics and lesion features of the study population are described in Table 1. All fractions were successfully delivered for 13 patients. As shown in Fig. 1, 2 subjects (patients 14 and 15) were excluded for technical reasons related to the impossibility of obtaining an external signal with the SGRT system. One patient (patient 16) was excluded because of a MANIV-induced gastric insufflation, which was detected on the first inter-arc cone beam CT of the first fraction. The stomach overfilling with air led to a cranial liver displacement with a supracentimetric magnitude. This phenomenon, illustrated in Fig. 3, was not observed on the planning CT. The treatment feasibility was, therefore, 92.9% (13/14).

The high-pressure level was 13 mbar, 16 mbar, 18 mbar, and 19 mbar for 1, 1, 9, and 2 patients, respectively. The low-pressure level was 0 mbar except for patient 6 for whom a positive end-expiratory pressure of 3 mbar was maintained because of severe chronic obstructive pulmonary disease (COPD). The average DIBH duration including the inspiratory and plateau phases was 27.1 (20.0-30.0) seconds, and the mean expiration time was 5.1 (4.2-5.7) seconds.

It was decided to abandon the use of SGRT to co-ordinate the beam delivery with mechanically induced DIBH. Indeed, the irradiation still continued during the early expiratory phase so that large deviations were imaged. An example is illustrated in Fig. E1. The mean percentage of aberrant target localizations in the total recorded positions was 5.7% (3.6%-8.9%) for patients 1, 2, and 3 in whom surface imaging was employed to automatically interrupt the beam. This proportion fell to 0.5% (0.0%-1.5%) because the treatment delivery was manually synchronized to the mechanical ventilator pressure curve. Target positions monitored during exhalation were not taken into account for safety margin calculation.

Random and systematic components of the interfraction repositioning error are detailed in Table E3. The error components of baseline shift and residual motion recalculated on the basis of intrafraction positional data are detailed in Table 2. Notably, the overall mean for the baseline shift was supramillimetric along the AP dimension of the liver tumors and was consequently added linearly to the margin. Considering an alpha coefficient of 2.5 and beta coefficient of 1.64, the safety margins for lung lesions were 4.6 mm/5.1 mm/5.6 mm in the LR, AP, and CC directions, respectively. Regarding liver malignancies, the PTV margins were 4.7 mm/7.3 mm/5.9 mm, respectively. Compared with PTV_{ITV} and PTV_{MidP}, the average reduction in irradiated volume with MANIV reached $-47.2\% \pm 15.3\%$, $P < .001$, and $-29.4\% \pm 19.2\%$, $P = .007$, for intrathoracic tumors and $-23.3\% \pm 12.4\%$, $P < .001$, and $-9.3\% \pm 15.3\%$, $P = .073$, for upper abdominal tumors, respectively. Beyond the statistical analysis, the decrease in the irradiated volume with MANIV increased with motion amplitude, as represented in Fig. E2. The percentiles of the target deviations measured during irradiation are summarized in Table 3. Their density plots are represented in Fig. 4. No fiducial migration was noticed between the planning CT acquisition and the treatment delivery. The lung geometric uncertainties were most pronounced in the CC direction. Concerning hepatic tumors, the deviations were also acceptable except for the large RDD caudal shift in patient 10, which was related to substantial intra-DIBH drifts. A sampled trajectory of the corresponding RDD during a VMAT arc is depicted in Fig. E3.

As listed in Table 4, an overall trend toward better OARs sparing was observed using MANIV-recalculated margins. Only the pulmonary dose metrics reached statistical significance for lung tumors. Regarding hepatic lesions, cardiac dose levels were significantly lower with mechanical ventilation compared with both free-breathing modalities as well as for the lungs in comparison with the ITV approach.

Table 1 Description of the study population and lesions features

Patient	Age	Gender+	ECOG status	BMI (kg/m²)	Cardiopulmonary	Others	Smoking status	Tumor diameter (mm)	Location	Histology	Fractionation schedule	LR	AP	CC	Fiducial
1	66	F	3	19.6	Stage III lung ADC.	Algodystrophy	Former	14	RUL	ADC†	5 × 11 Gy	5.0	5.9	6.5	Visicoil (0.75 × 10 mm)
2	67	F	0	21.0	Stage IV lung ADC (multiple nodules)	-	Active	13	LLL	SCLC†	5 × 11 Gy	1.5	4.2	13.0	Visicoil (0.75 × 10 mm)
								16	RLL	ADC†	5 × 11 Gy	5.1	8.2	21.8	Visicoil (0.75 × 10 mm)
3	76	M	1	19.2	COPD Gold II	Diffuse atheromatous stenosis	Active	42	RUL	SCC†	5 × 11 Gy	4.0	3.9	1.1	Visicoil (0.75 × 10 mm)
4	75	F	1	29.7	HBP	Hypothyroidism	Former	26	LUL	ADC†	5 × 11 Gy	2.6	5.3	5.5	Visicoil (0.75 × 10 mm)
5	70	F	1	22.1	COPD Gold II		Active	12	LLL	SCLC†	4 × 12 Gy	2.8	4.4	20.9	Visicoil (0.5 × 10 mm)
6	70	F	1	19.4	COPD Gold III. HBP	AAA. PMR	Former	17	RLL	Unknown†	4 × 12 Gy	4.1	11.0	12.3	Surgical clip
7	58	M	0	36.2	-	Alcoholic cirrhosis (Child-Pugh A5). Portal hypertension. Esophageal varices. DM type II	Never	25	S VIII	HCC†	5 × 10 Gy	4.0	8.3	20.6	Lipiodol
8	77	M	1	19.6	DCM. Aortic regurgitation	-	Never	23	SIV-SVII	ADC	5 × 10 Gy	2.3	2.8	5.6	Surgical clip
								24	SIV-SVIII	ADC	5 × 10 Gy	7.6	7.5	8.2	Surgical clip
9	95	M	1	24.2	. 2nd degree AVB (pacemaker)	Hepatitis B	Former	39	SIV-SVIII	HCC†	5 × 10 Gy	1.6	8.0	12.6	Surgical clip
10	58	M	0	28.6	-	Hypothyroidism	Never	24	SS	ADC	5 × 10 Gy	2.4	4.5	11.0	Surgical clip
11	74	M	1	25.4	HBP	Hemochromatosis. RA. ESRD	Former	35	S VII	HCC†	5 × 10 Gy	5.8	5.5	30.7	None
12*	58	F	1	34.5	-	Alcoholic cirrhosis (Child-Pugh A6). Portal hypertension. Esophageal varices. DM type II	Active	32	SVIII	HCC†	5 × 10 Gy	3.8	3.8	11.5	Spi Balt (0.36 × 4 mm)
13	53	F	0	39.0	-	Crohn disease. HBP	Never	50	SVII	ADC	5 × 10 Gy	3.9	4.3	16.1	None
14	68	F	0	19.2	-	Hyperparathyroidism. Hypothyroidism	Never	22	SIV	ADC	6 × 8 Gy	3.4	7.4	17.8	Spi Balt (0.36 × 4 mm)
15	56	M	0	32.1	Hepatitis B. HBP	-	Never	10	SI	HCC†	5 × 10 Gy	1.7	4.8	9.4	Spi Balt® (0.36 × 4 mm)
16	62	M	0	28.0	-	Portal vein thrombosis. DM type II	Never	20	SS	CHC†	5 × 10 Gy	1.0	10.5	19.6	Surgical clip

Abbreviations: AAA = abdominal aortic aneurysm; ADC = adenocarcinoma; ADC = adenocarcinoma; AP = anteroposterior; AVB = atrioventricular block; BMI = body mass index; CC = craniocaudal; CHC = cholangiocarcinoma; COPD = chronic obstructive pulmonary disease; DCM = dilated cardiomyopathy; DM = diabetes mellitus; ECOG = eastern cooperative oncology group; ESRD = end stage renal disease; HBP = high blood pressure; HCC = hepatocarcinoma; LLL = left lower lobe; LR = left-right; LUL = left upper lobe; PMR = polymyalgia rheumatica; RA = rheumatoid arthritis; RLL = right lower lobe; RUL = right upper lobe; SCC = squamous cell carcinoma; SCLC = small cell lung carcinoma; SS = surgical section.

*Abdominal compression applied.

†Primary lesion.

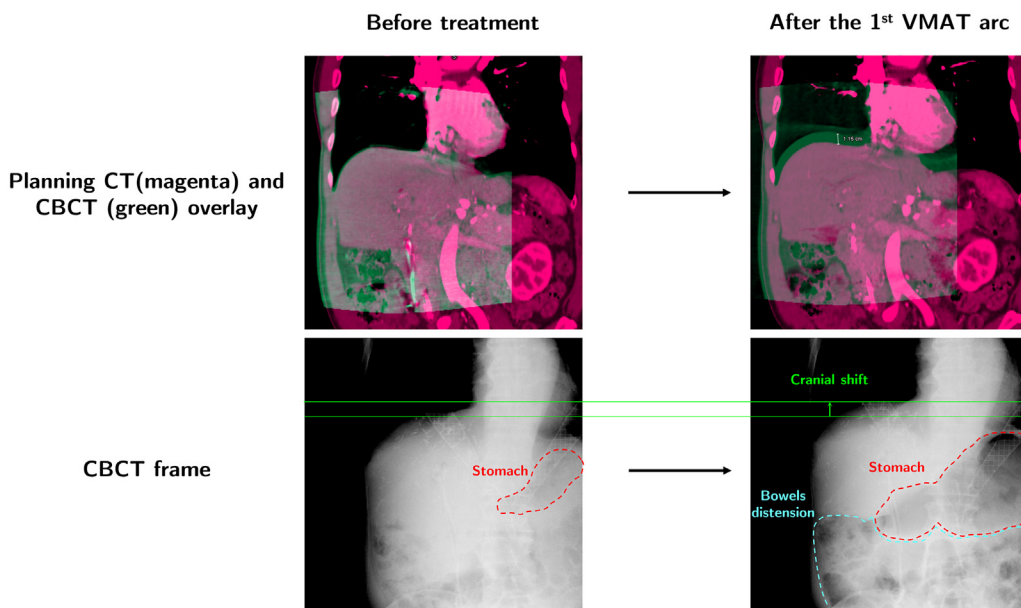+ Female (F) and Male (M) refer to XX and XY karyotypes, respectively.

Before treatment   **After the 1ˢᵗ VMAT arc**

Figure 3   Gastric insufflation in patient 16 leading to a major cranial shift of the liver.
Abbreviations: CBCT = cone beam computed tomography, VMAT = volumetric modulated arc therapy.

The total slot time was on average 53.1 ± 10.6 minutes. The time needed for tumor-based repositioning before the first arc was 6.1 ± 2.8 minutes, whereas the cone beam CT-based inter-arc matching procedure took an average of 14.4 ± 5.8 minutes. The average irradiation time was 9.3 ± 2.0 minutes. The total slot time as a function of the fraction number is represented in Fig. E4.

The mean global tolerance score to treatment was 3.8 ± 0.6 and did not differ significantly between patients with thoracic or abdominal tumors: 3.8 ± 0.6 versus 3.9 ± 0.7, $P = .753$. The DIBH comfort level was $80.1\% \pm 10.6\%$ and was also comparable between SBRT sites: $79.0\% \pm 8.1\%$ versus $81.1\% \pm 8.2\%$, $P = .723$. No adverse event and no abnormal vital parameter values were noticed.

At a median follow-up of 15 (2-26) months, 2 local failures occurred (patients 8 and 13). Because patient 7 underwent a liver transplant a few weeks after completing SBRT, the local control was not applicable. Patients 3 and 11 died at 2 and 5 months of follow-up, respectively, for reasons unrelated to their radiation therapy treatment.

Discussion

In an unselected population representative of the patient profiles encountered in clinical routine, excellent treatment feasibility was achieved with mechanical ventilation. In addition, the treatment tolerance was better than acceptable with a highly reassuring safety profile. Moreover, the mechanical ventilator used for this protocol is already fully approved for clinical use. Hence, one does not have to prototype a dedicated ventilation system and can directly start with a device that is being used routinely by other departments with all the safety guarantees. Notwithstanding, motion management of patient 16 was converted to the conventional margin approach because of gastric insufflation with a major impact on the target position. In the context of the common use of noninvasive mechanical ventilation, its incidence varies from 5% to 30%-40% and occurs when the positive pressure becomes larger than the resistance capacity of the lower esophageal sphincter (20-25 mbar in adults).[30] For patient 16, the high-pressure level was 18 mbar. In short, a compromise must be found between a pressure that is not excessive, in

Table 2   **Errors components of residual motion and baseline shift with MANIV**

	Residual errors					
	Lung			Liver		
	LR	AP	CC	LR	AP	CC
M (mm)	0.2	−0.3	0.06	0.1	−1.3	0.7
Baseline shift						
σ (mm)	1.0	1.6	1.6	1.4	1.6	1.2
Σ (mm)	1.1	1.1	1.4	0.3	1.1	1.3
Residual motion						
σ (mm)	0.7	1.0	1.5	-	-	2.0

Abbreviations: AP = anteroposterior; CC = Craniocaudal; MANIV = mechanically assisted and noninvasive ventilation; LR = left-right.

Table 3   **Percentiles of deviations per patient***

Percentiles of deviations					
3-dimensional magnitude deviations					
Patients	**Percentile 50%**	**Percentile 70%**	**Percentile 80%**	**Percentile 90%**	**Percentile 95%**	**Percentile 98%**
Patient 1	2.8 mm	3.1 mm	3.4 mm	3.7 mm	4.3 mm	5.2 mm
Patient 2†	2.6 mm	3.2 mm	3.7 mm	4.3 mm	4.9 mm	5.4 mm
Patient 2‡	2.8 mm	3.5 mm	4.1 mm	4.8 mm	5.4 mm	6.1 mm
Patient 3	2.9 mm	3.7 mm	4.1 mm	4.6 mm	5.1 mm	5.7 mm
Patient 4	2.0 mm	2.4 mm	2.7 mm	3.1 mm	3.4 mm	3.9 mm
Patient 5	3.0 mm	3.8 mm	4.4 mm	5.2 mm	5.9 mm	6.9 mm
Craniocaudal deviations					
Patients	**Percentile 50%**	**Percentile 70%**	**Percentile 80%**	**Percentile 90%**	**Percentile 95%**	**Percentile 98%**
Patient 6	3.8 mm	5.2 mm	5.7 mm	6.3 mm	6.7 mm	7.0 mm
Patient 7	1.2 mm	1.8 mm	2.3 mm	3.1 mm	3.8 mm	4.6 mm
Patient 8	1.9 mm	3.0 mm	4.2 mm	6.0 mm	7.6 mm	8.8 mm
Patient 9	1.3 mm	2.0 mm	2.7 mm	3.7 mm	4.4 mm	4.8 mm
Patient 10	5.9 mm	7.9 mm	8.8 mm	9.9 mm	10.6 mm	11.5 mm
Patient 11	1.2 mm	1.9 mm	2.3 mm	2.9 mm	3.6 mm	4.3 mm
Patient 13	2.1 mm	4.0 mm	4.9 mm	6.0 mm	6.5 mm	7.1 mm

*Patients 1 to 6 had lung lesions. Patients 7 to 13 received diagnoses of hepatic tumors.
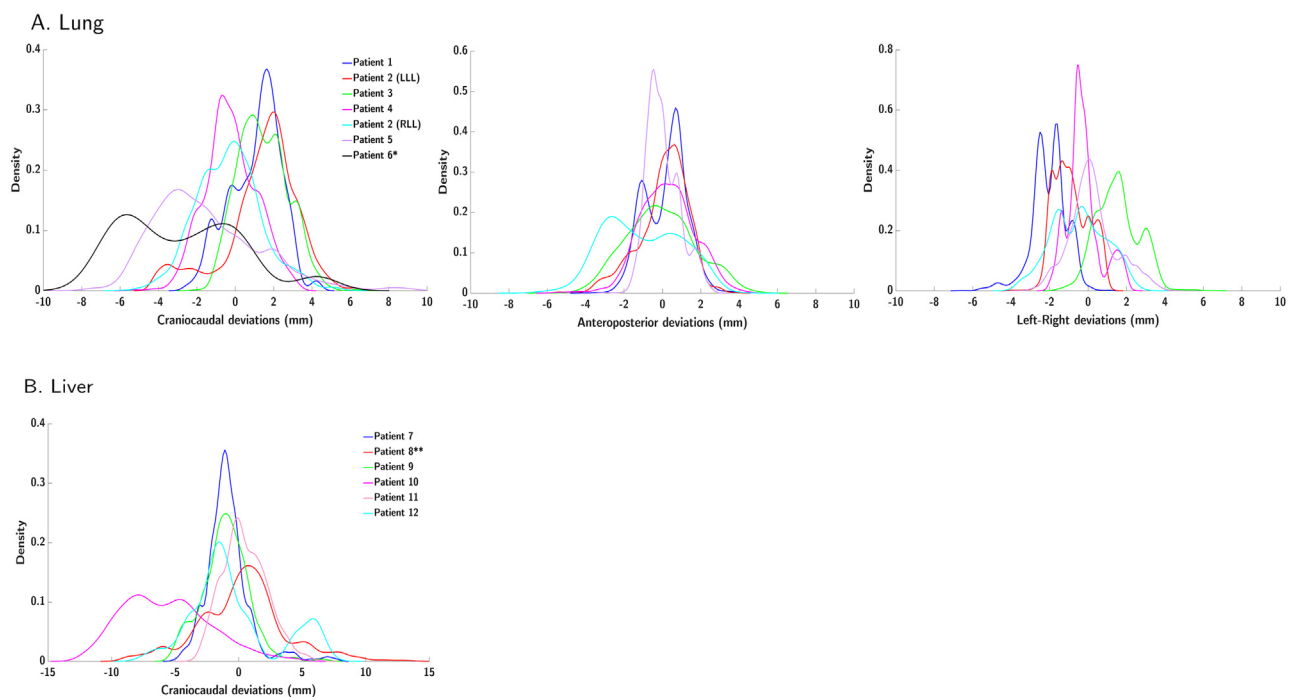†Left lower lobe lesion.
‡Right lower lobe lesion.

Figure 4   Density plot of the intrafraction deviations measured during the whole treatment course for each patient. *For patient 6, the target deviations were only monitored along the craniocaudal dimension. **For patient 8, only 1 deviation curve is displayed because the 2 lesions were treated simultaneously.
Abbreviations: LLL = left lower lobe; RLL = right lower lobe.

Table 4   Mean values of the dose metrics for tumors and organs at risk

	Lung (n = 7)					Liver (n = 10)				
	ITV	*P* value[†]	MidP	*P* value[‡]	MANIV	ITV	*P* value[†]	MidP	*P* value[‡]	MANIV
PTV										
$D_{99\%}$ (Gy)	51.5 ± 3.9	.222	51.6 ± 4.1	.315	51.9 ± 4.5	40.5 ± 9.8	0.114	40.5 ± 12.5	0.721	41.0 ± 10.9
$D_{95\%}$ (Gy)	53.7 ± 4.3	.131	53.8 ± 4.5	.498	53.7 ± 4.3	43.9 ± 9.4	0.482	43.9 ± 10.5	0.240	44.9 ± 8.7
$D_{2\%}$ (Gy)	63.0 ± 4.4	.338	64.3 ± 4.6	.167	63.6 ± 4.1	59.8 ± 2.3	0.954	59.2 ± 3.7	0.484	59.8 ± 2.1
D_{mean} (Gy)	58.4 ± 3.9	.433	58.6 ± 3.2	.052	58.2 ± 3.4	52.9 ± 2.9	0.959	52.8 ± 2.8	0.499	53.2 ± 2.7
Heart										
D_{mean} (Gy)	0.5 ± 0.6	.018	0.7 ± 0.6	.036	0.4 ± 0.4	2.0 ± 1.5	0.007*	1.8 ± 1.5	0.005*	1.1 ± 1.4
$D_{2\%}$ (Gy)	2.7 ± 2.7	.043	2.7 ± 2.6	.136	2.0 ± 1.6	9.5 ± 7.8	0.004*	8.2 ± 6.4	0.005*	5.1 ± 6.0
Lungs										
D_{mean} (Gy)	2.6 ± 1.1	< .001*	2.3 ± 0.8	.002*	1.9 ± 0.8	3.0 ± 1.7	0.005*	2.5 ± 1.4	0.060	2.0 ± 1.1
V_{20Gy} (%)	3.5 ± 1.7	.005*	2.8 ± 1.2	< .001*	2.1 ± 1.3	4.4 ± 3.3	0.008*	3.0 ± 2.4	0.109	2.1 ± 1.9
Spinal cord										
$D_{2\%}$ (Gy)	7.9 ± 6.2	.219	7.9 ± 4.6	.08	6.7 ± 4.6	6.3 ± 5.0	0.139	7.1 ± 4.5	0.048	5.6 ± 3.9
Chest wall										
V_{30Gy} (cc)	25.9 ± 20.0	.028	15.9 ± 15.2	.764	14.5 ± 14.1	39.8 ± 61.2	0.150	25.6 ± 40.8	0.463	23.4 ± 46.0
Great vessels										
$D_{2\%}$ (Gy)	13.5 ± 13.4	.086	13.5 ± 12.9	.046	11.5 ± 11.5	28.3 ± 17.3	0.629	27.2 ± 16.2	0.994	27.1 ± 15.5
Oesophagus										
$D_{2\%}$ (Gy)	5.8 ± 5.8	.063	5.8 ± 3.9	.013	3.3 ± 2.6	9.2 ± 7.8	0.120	10.4 ± 7.4	0.092	7.2 ± 5.5
Bronchial tree										
$D_{2\%}$ (Gy)	3.7 ± 3.6	.816	4.1 ± 3.9	.043	3.7 ± 3.4	-	-	-	-	-
Stomach										
$D_{2\%}$ (Gy)	-	-	-	-	-	9.1 ± 9.3	0.431	9.4 ± 8.4	0.407	7.6 ± 6.2
Duodenum										
$D_{2\%}$ (Gy)	-	-	-	-	-	4.9 ± 7.1	0.721	4.4 ± 6.3	0.266	7.7 ± 9.3
Liver										
$D_{\geq 700\ cm^3}$ (Gy)	-	-	-	-	-	7.7 ± 5.9	0.063	5.5 ± 3.9	0.646	5.1 ± 3.5
V_{10Gy} (%)	-	-	-	-	-	37.8 ± 9.7	0.081	32.7 ± 9.6	0.857	32.1 ± 12.6
D_{mean} (Gy)	-	-	-	-	-	11.8 ± 3.0	0.023	10.3 ± 2.7	0.324	9.7 ± 3.0
Kidney										
D_{mean} (Gy)	-	-	-	-	-	2.9 ± 4.1	0.445	2.4 ± 3.7	0.457	2.6 ± 3.4
Colon										
$D_{2\%}$ (Gy)	-	-	-	-	-	4.0 ± 4.4	0.878	4.3 ± 5.9	0.799	3.4 ± 3.6

ITV = internal target volume; MANIV = mechanically assisted and noninvasive ventilation; MidP = mid-position; PTV = planning target volume.
*P values that reached statistical significance.
†P values for ITV versus MANIV values.
‡P values for MidP versus MANIV values.

order to avoid this complication, but high enough to effectively constrain the maintenance of reproducible BHs.

The time efficiency of irradiation was ensured by the uninterrupted sequence of apneas without free-breathing intervals. By subtracting the duration of the study-specific inter-arc matching procedure, about 38.3 ± 6.3 minutes were required on average, which seem compatible with clinical routine. To this, approximately 1 minute of free-breathing recovery time must be added between each arc. For patient 6, this pause was

respected in the middle of each arc because of COPD severity.

With respect to intrafraction deviations, good positional reproducibility of the lung lesions was noticed without the need for additional real-time imaging with implanted fiducials. Consequently, MANIV allowed for a noteworthy reduction in the irradiated volume compared with standard free-breathing techniques. Although only statistically significant for the lungs, a better overall dosimetric sparing was found. These results pave the way for extending MANIV indications to patients who received diagnoses of locally advanced lung carcinoma and were eligible for chemoradiotherapy in whom a more clinically meaningful difference in OARs dose is expected between treatment modalities. Regarding upper abdominal lesions, the bulk of the RDD deviation distribution was in line with the proposed craniocaudal margin with the exception of patient 10 for whom considerable motion was noted. Such large intra-BH movement has already been reported during voluntary[14,31] and spirometer-enhanced[13] apneas. Remarkably, the tumor drift was documented as moving cranially, whereas caudal drifts were observed for patient 10.

Voluntary DIBH appears to be a competitor to MANIV-induced DIBH. Unfortunately, the noncomparative design of the study prevented a direct confrontation between both techniques. Although superiority cannot be established, treatment feasibility with MANIV was in the upper limit of the range reported in the literature for voluntary DIBH, which varies from 72% to 94%.[16,32-35] However, the small sample size should prompt caution in generalizing the data of the present study. The comfort level with MANIV in this trial was almost identical to that reported for voluntary DIBH among patients with breast cancer for whom a similar evaluation method was used.[21] Finally, substantial intra-BH drift was measured in 16.7% (1/6) of liver lesions with MANIV. Stick et al[14] monitored intrafraction residual motion with fluoroscopy during voluntary DIBH in 4 patients with hepatic neoplasia. For 50% of them, supracentimetric tumor drifts were measured. Lens et al[13] reported comparable values for 20% (2/10) of patients with pancreatic tumors. However, it should be noted that the latter analysis involved 3 fractions out of 13 to 20 depending on the fractionation scheme. Concerning thoracic malignancies, most of the studies estimating the geometric uncertainties during voluntary[16,33,36] or spirometer-guided[34,36,37] BHs showed comparable results with MANIV-induced DIBH. However, their methods were based on static images acquired over a limited number of apneas. Therefore, the range of deviations represented only a part of the picture and neglected the tumor stability while supracentimetric intra-apnea drift may occur.[15] Scherman Rydhög et al[12] demonstrated good positional reproducibility and stability of lung lesions during voluntary DIBH quantified, for the first time, by fluoroscopy. The vast majority of deviations were indeed less than 5 mm. Yet, all lesions were located in the upper lobe, which is known to exhibit better repositioning than the lower lobe.[36] Hoffman et al[38] reported systematic and random components of baseline shift during voluntary DIBH along the 3 dimensions, which were all larger than those of MANIV, except for Σ in LR. We believe that an important avenue of investigation would consist of an extensive fluoroscopic and intrairradiation assessment of tumor deviations during voluntary DIBH for all fractions. This would allow a more comprehensive estimate of geometric uncertainties.

Continuous positive airway pressure (CPAP) is a method similar to MANIV in the sense that the effects of the technique are mediated by positive pressure. There are also notable distinctions that should be mentioned: the pressure is applied continuously and is generally lower than MANIV with a maximum of 15 mbar. In free breathing, CPAP actively mitigates the tumor motion amplitude, lowering the PTV_{ITV} volume by 19% to 27%.[39,40] The feasibility of combining CPAP and DIBH was recently demonstrated in a retrospective study.[41] However, patients with cardiopulmonary comorbidities were excluded, and intrafraction motion monitoring was not carried out. We thus believe that a prospective comparison of the positional stability and reproducibility of mobile tumors between MANIV and CPAP in an unselected population is an interesting perspective.

This study has several limitations. First, this work involved a limited number of patients from a single institution. Second, motion analysis methods were not uniform between lung and liver lesions. They also differed within the 2 groups of lesions. This may have degraded the uncertainty estimation's accuracy for both tumor locations and also limited their comparability. In addition, the deviations of the intrapulmonary gold fiducials from their reference position on the planning CT could have incorporated some setup errors. It is, therefore, possible that the PTV margin was overvalued. The RDD was tracked instead of radiopaque markers implanted within the liver lesions. Conversely, it has been shown to be a reliable indicator of hepatic tumor movement.[42,43]

Conclusions

Mechanical ventilation achieves high treatment feasibility even in the presence of severe comorbidities without prohibitively affecting patient comfort. The positional stability and reproducibility of pulmonary tumors during MANIV-induced DIBH are good and allow a significant reduction in irradiated volume compared with traditional free-breathing radiation therapy. The same is true for liver lesions, although substantial deviations are possible. Routine treatment of upper abdominal lesions, therefore, requires precautions such as pretreatment verification of

diaphragm stability by fluoroscopy and prevention of the risk of gastric insufflation.

Disclosures

None.

Acknowledgments

Supplementary materials

Supplementary material associated with this article can be found in the online version at doi:10.1016/j.adro. 2024.101563.

References

1. Brandner ED, Chetty IJ, Giaddui TG, Xiao Y, Huq MS. Motion management strategies and technical issues associated with stereotactic body radiotherapy of thoracic and upper abdominal tumors: A review from NRG oncology. *Med Phys*. 2017;44(6):2595-2612.
2. Wolthaus JWH, Sonke JJ, van Herk M, et al. Comparison of different strategies to use four-dimensional computed tomography in treatment planning for lung cancer patients. *Int J Radiat Oncol Biol Phys*. 2008;70(4):1229-1238.
3. Ball HJ, Santanam L, Senan S, Tanyi JA, van Herk M, Keall PJ. Results from the AAPM Task Group 324 respiratory motion management in radiation oncology survey. *J Appl Clin Med Phys*. 2022;23(11):e13810. https://doi.org/10.1002/acm2.13810.
4. Anastasi G, Bertholet J, Poulsen P, et al. Patterns of practice for adaptive and real-time radiation therapy (POP-ART RT) part I: Intra-fraction breathing motion management. *Radiother Oncol*. 2020;153:79-87.
5. Vander Veken L, Dechambre D, Sterpin E, et al. Incorporation of tumor motion directionality in margin recipe: The directional MidP strategy. *Phys Med*. 2021;91:43-53.
6. Wanet M, Sterpin E, Janssens G, Delor A, Lee JA, Geets X. Validation of the mid-position strategy for lung tumors in helical TomoTherapy. *Radiother Oncol*. 2014;110(3):529-537.
7. Lens E, van der Horst A, Versteijne E, van Tienhoven G, Bel A. Dosimetric advantages of midventilation compared with internal target volume for radiation therapy of pancreatic cancer. *Int J Radiat Oncol Biol Phys*. 2015;92(3):675-682.
8. Jin P, Machiels M, Crama KF, et al. Dosimetric benefits of midposition compared with internal target volume strategy for esophageal cancer radiation therapy. *Int J Radiat Oncol Biol Phys*. 2019;103(2):491-502.
9. Dechambre D, Vander Veken L, Delor A, Sterpin E, Vanneste F, Geets X. Feasibility of a TPS-integrated method to incorporate tumor motion in the margin recipe. *Med Dosim*. 2021;46(3):253-258.
10. Dhont J, Vandemeulebroucke J, Burghelea M, et al. The long- and short-term variability of breathing induced tumor motion in lung and liver over the course of a radiotherapy treatment. *Radiother Oncol*. 2018;126(2):339-346.
11. Bertholet J, Knopf A, Eiben B, et al. Real-time intrafraction motion monitoring in external beam radiotherapy. *Phys Med Biol*. 2019;64 (15):15TR01.
12. Scherman Rydhög J, Riisgaard de Blanck S, Josipovic M, et al. Target position uncertainty during visually guided deep-inspiration breath-hold radiotherapy in locally advanced lung cancer. *Radiother Oncol*. 2017;123(1):78-84.
13. Lens E, van der Horst A, Versteijne E, Bel A, van Tienhoven G. Considerable pancreatic tumor motion during breath-holding. *Acta Oncol*. 2016;55(11):1360-1368.
14. Stick LB, Vogelius IR, Risum S, Josipovic M. Intrafractional fiducial marker position variations in stereotactic liver radiotherapy during voluntary deep inspiration breath-hold. *Br J Radiol*. 2020;93(1116): 20200859.
15. Kamima T, Iino M, Sakai R, et al. Evaluation of the four-dimensional motion of lung tumors during end-exhalation breath-hold conditions using volumetric cine computed tomography images. *Radiother Oncol*. 2023;182:109573.
16. Josipovic M, Aznar MC, Thomsen JB, et al. Deep inspiration breath hold in locally advanced lung cancer radiotherapy: validation of intrafractional geometric uncertainties in the INHALE trial. *Br J Radiol*. 2019;92(1104):20190569.
17. Parkes MJ, Green S, Stevens AM, Parveen S, Stephens R, Clutton-Brock TH. Reducing the within-patient variability of breathing for radiotherapy delivery in conscious, unsedated cancer patients using a mechanical ventilator. *Br J Radiol*. 2016;89(1062):20150741.
18. Van Ooteghem G, Dasnoy-Sumell D, Lee JA, Geets X. Mechanically-assisted and non-invasive ventilation for radiation therapy: A safe technique to regularize and modulate internal tumour motion. *Radiother Oncol*. 2019;141:283-291.
19. Van Ooteghem G, Dasnoy-Sumell D, Lambrecht M, et al. Mechanically-assisted non-invasive ventilation: A step forward to modulate and to improve the reproducibility of breathing-related motion in radiation therapy. *Radiother Oncol*. 2019;133:132-139.
20. West NS, Parkes MJ, Snowden C, et al. Mitigating respiratory motion in radiation therapy: rapid, shallow, non-invasive mechanical ventilation for internal thoracic targets. *Int J Radiat Oncol Biol Phys*. 2019;103(4):1004-1010.
21. Vander Veken L, Van Ooteghem G, Razavi A, et al. Voluntary versus mechanically-induced deep inspiration breath-hold for left breast cancer: a randomized controlled trial. *Radiother Oncol*. 2023;183:109598.
22. van Herk M, Remeijer P, Rasch C, Lebesque JV. The probability of correct target dosage: dose-population histograms for deriving treatment margins in radiotherapy. *Int J Radiat Oncol Biol Phys*. 2000;47 (4):1121-1135.
23. Sonke JJ, Rossi M, Wolthaus J, van Herk M, Damen E, Belderbos J. Frameless stereotactic body radiotherapy for lung cancer using four-dimensional cone beam CT guidance. *Int J Radiat Oncol Biol Phys*. 2009;74(2):567-574.
24. Case RB, Sonke JJ, Moseley DJ, Kim J, Brock KK, Dawson LA. Inter- and intrafraction variability in liver position in non−breath-hold stereotactic body radiotherapy. *Int J Radiat Oncol Biol Phys*. 2009;75 (1):302-308.
25. Diez P, Hanna GG, Aitken KL, et al. UK 2022 consensus on normal tissue dose-volume constraints for oligometastatic, primary lung and hepatocellular carcinoma stereotactic ablative radiotherapy. *Clin Oncol*. 2022;34(5):288-300.
26. Poulsen PR, Cho B, Keall PJ. A method to estimate mean position, motion magnitude, motion correlation, and trajectory of a tumor from cone-beam CT projections for image-guided radiotherapy. *Int J Radiat Oncol Biol Phys*. 2008;72(5):1587-1596.
27. Vander Veken L, Dechambre D, Michiels S, et al. Improvement of kilovoltage intrafraction monitoring accuracy through gantry angles selection. *Biomed Phys Eng Express*. 2020;6(6): 065002.

28. A'Hern RP. Sample size tables for exact single-stage phase II designs. *Stat Med*. 2001;20(6):859-866.

29. Benjamini Y, Hochberg Y. Controlling the false discovery rate: a practical and powerful approach to multiple testing. *J R Stat Soc Ser B Methodol*. 1995;57(1):289-300.

30. Carron M, Freo U, BaHammam AS, et al. Complications of non-invasive ventilation techniques: a comprehensive qualitative review of randomized trials. *Br J Anaesth*. 2013;110(6):896-914.

31. Lens E, Gurney-Champion OJ, Tekelenburg DR, et al. Abdominal organ motion during inhalation and exhalation breath-holds: pancreatic motion at different lung volumes compared. *Radiother Oncol*. 2016;121(2):268-275.

32. Giraud P, Morvan E, Claude L, et al. Respiratory gating techniques for optimization of lung cancer radiotherapy. *J Thorac Oncol Off Publ Int Assoc Study Lung Cancer*. 2011;6(12):2058-2068.

33. Josipovic M, Persson GF, Dueck J, et al. Geometric uncertainties in voluntary deep inspiration breath hold radiotherapy for locally advanced lung cancer. *Radiother Oncol*. 2016;118(3):510-514.

34. Brock J, McNair HA, Panakis N, Symonds-Tayler R, Evans PM, Brada M. The use of the active breathing coordinator throughout radical Non−Small-Cell Lung Cancer (NSCLC) radiotherapy. *Int J Radiat Oncol*. 2011;81(2):369-375.

35. Peeters STH, Vaassen F, Hazelaar C, et al. Visually guided inspiration breath-hold facilitated with nasal high flow therapy in locally advanced lung cancer. *Acta Oncol*. 2021;60(5):567-574.

36. Prado A, Zucca D, De La, Casa MÁ, et al. Intrafraction target shift comparison using two breath-hold systems in lung stereotactic body radiotherapy. *Phys Imaging Radiat Oncol*. 2022;22:57-62.

37. Den Otter LA, Kaza E, Kierkels RGJ, et al. Reproducibility of the lung anatomy under active breathing coordinator control: Dosimetric consequences for scanned proton treatments. *Med Phys*. 2018;45 (12):5525-5534.

38. Hoffmann L, Ehmsen Ml, Hansen J, et al. Repeated deep-inspiration breath-hold CT scans at planning underestimate the actual motion between breath-holds at treatment for lung cancer and lymphoma patients. *Radiother Oncol*. 2023;188: 109887. https://doi.org/10.1016/j.radonc.2023.109887.

39. Goldstein JD, Lawrence YR, Appel S, et al. Continuous positive airway pressure for motion management in stereotactic body radiation therapy to the lung: a controlled pilot study. *Int J Radiat Oncol Biol Phys*. 2015;93(2):391-399.

40. Jacobson G, Lawrence YR, Appel S, et al. Benefits of continuous positive airway pressure (CPAP) during radiation therapy: a prospective Trial. *Int J Radiat Oncol Biol Phys*. 2021;110 (5):1466-1472.

41. Appel S, Lawrence YR, Bar J, et al. Deep inspiratory breath hold assisted by continuous positive airway pressure ventilation for lung stereotactic body radiotherapy. *Cancer/Radiothérapie*. 2023;27(1):23-30.

42. Veldman JK, Van Kesteren Z, Gunwhy ER, et al. Accuracy of abdominal organ motion estimation in radiotherapy using the right hemidiaphragm top as a surrogate during prolonged breath-holds quantified with MRI. *Med Phys*. 2023;50(6):3299-3310.

43. Yang J, Cai J, Wang H, et al. Is diaphragm motion a good surrogate for liver tumor motion? *Int J Radiat Oncol Biol Phys*. 2014;90(4):952-958.